JOURNAL OF APPLIED ELECTROCHEMISTRY 18 (1988) 857–862

Electrochemical characteristics and structural changes of molybdenum trioxide hydrates as cathode materials for lithium batteries*

NAOAKI KUMAGAI, NOBUKO KUMAGAI, KAZUO TANNO

Department of Applied Chemistry, Faculty of Engineering, Iwate University, Morioka, 020, Japan

Received 25 January 1988; revised 19 April 1988

Several characteristics of $MoO_3 \cdot 2H_2O$ and $MoO_3 \cdot H_2O$, such as thermal behaviour and conductivity and the electrochemical behaviour and structural changes associated with discharge and charge have been investigated. The suitability of these substances as new cathode materials for non-aqueous lithium batteries has been assessed. $MoO_3 \cdot H_2O$, having only one coordinated water molecule, showed a discharge capacity of about 400 Ah kg^{-1} of acid weight and a discharge potential around 2.5 V vs Li/Li^+. This capacity was much higher than the 280 Ah kg^{-1} of anhydrous MoO_3. $MoO_3 \cdot H_2O$ showed good charge–discharge cyclic behaviour at a capacity below 1 e^-/Mo while keeping the original layered lattice on cycling. In addition, the crystal system of $MoO_3 \cdot H_2O$ was found to be changed from a monoclinic system to orthorhombic with lattice parameters of $a = 0.5285$ nm, $b = 1.0824$ nm, $c = 0.5237$ nm on discharge to 0.5 e^-/Mo.

1. Introduction

Non-aqueous lithium batteries based on topochemical reactions are currently of great interest as power sources with high energy density. Several molybdenum oxides [1–3], such as MoO_3, Mo_8O_{52}, Mo_8O_{23} and $Mo_{17}O_{47}$, have been investigated as cathode materials because of the high energy density of lithium–molybdenum oxide cells.

In our previous paper [4], the electrochemical and structural characteristics of the molybdic acid C phase containing a small amount of ammonium ion $x[(NH_4)_2O] \cdot MoO_3 \cdot y(H_2O)$ ($x = 0.075$–0.042, $y = 0.400$–0.043), were investigated, and it was shown that the molybdic acid C phase had a high discharge capacity of 390–460 Ah/kg-acid weight and the capacity increased with decreasing y value. In this paper, several characteristics of molybdenum trioxide hydrates or molybdic acids, $MoO_3 \cdot 2H_2O$ and $MoO_3 \cdot H_2O$, such as thermal behaviour and conductivity were investigated together with their electrochemical behaviour. Structural changes associated with discharge and recharge were also investigated when the materials were employed as cathode materials in lithium cells.

2. Experimental details

Molybdenum trioxide dihydrate and its monohydrate (yellow) were prepared according to the method of Freedmann [5]. The molybdic acid C phase was prepared according to Peters *et al.* [6]. Preparation of

Table 1. Preparation and characteristics of various molybdenum oxides

Number	*Compound*	*Preparation*	*Conductivity* ($\Omega^{-1}cm^{-1}$ at 25° C)	*Colour*
1	$MoO_3 \cdot 2H_2O$	Acidification of Na_2MoO_4 solution	$\sim 7.0 \times 10^{-10}$	Yellow
2	$MoO_3 \cdot H_2O$	Heat treatment of 1 at 80° C for 3 h	$\sim 6.3 \times 10^{-10}$	Bright yellow
3	MoO_3	Heat treatment of 1 at 500° C for 3 h	$\sim 5.3 \times 10^{-11}$	Pale blue
4	$0.075[(NH_4)_2O] \cdot MoO_3 \cdot 0.40(H_2O)$	Acidification of $(NH_4)_6Mo_7O_{24}$ solution	$\sim 1.0 \times 10^{-9}$	Pale blue
5	$0.073[(NH_4)_2O] \cdot MoO_3 \cdot 0.092(H_2O)$	Heat treatment of 4 at 200° C for 3 h	$\sim 4.5 \times 10^{-9}$	Light grey
6	MoO_3	Heat treatment of 4 at 500° C for 3 h	$\sim 1.3 \times 10^{-8}$	Grey

* This paper was originally presented at the Fall 1987 Meeting of the Electrochemical Society, Inc. held at Honolulu, Hawaii (Proceedings of the Symposium on Primary and Secondary Ambient Temperature Batteries, PV88-6, p. 484–493 (1987).

0021-891X/88 $03.00 + .12

these compounds is summarized in Table 1. The prepared compounds were identified by X-ray diffractometry, infrared (IR) spectroscopy and chemical analysis.

The X-ray diffraction measurement was conducted using a Rigaku Denki Guigerflex 20B and CuKα radiation and thermogravimetric analysis was made using a Rigaku Denki TG-DTA machine. The IR spectrum was recorded on a Hitachi 295 IR spectrophotometer with a KBr disc method. Conductivity measurements were made on the pellets with a blocking silver electrode by means of an a.c. impedance technique, using a computer NF Electronic Instrument S-5720B frequency response analyser. The frequency range was usually 10 mHz to 10 kHz, and 1 V r.m.s. amplitude signal was applied. The pellets were obtained by compression-moulding the molybdenum oxide powder under 90 MPa at room temperature. Conductivity was extracted by plotting the data in the complex impedance plane in the usual way [7].

Preparation of electrodes and the electrolyte and cell assembly were carried out in the same way as described in previous papers [8, 9]. The mixture of the molybdenum compound and graphite as a conducting agent, in a weight ratio of 1 : 1, was compression moulded on a nickel net under 50 MPa. The pellet thus obtained was used as a cathode after drying under vacuum at 25° C for one day. The apparent surface area of the cathode was 1.3 cm^2, and the weights of the cathodes were about 30 mg. Lithium pellets, cut from a lithium block, were used as an anode and as a reference electrode. The electrolyte used was 1.0 M $LiClO_4$ in propylene carbonate (PC), butyrolacetone (BL) and dimethyl sulphoxide (DMSO), all of which contained only trace amounts of water of less than 100 mg dm^{-3}. Cell assembly was as follows: one cathode was wrapped in non-woven polypropylene, which was sandwiched between two lithium anodes. The element was then inserted into a glass-beaker type cell case and the cell was filled with about 20 ml of electrolyte solution.

3. Results and discussion

3.1. *Characteristics of molybdenum oxide hydrates and their heated products*

Thermogravimetric curves of $MoO_3 \cdot 2H_2O$ (number 1 in Table 1) and the molybdic acid C phase (number 4) are shown in Fig. 1. It can be seen from Fig. 1 that dehydration of the dihydrate takes place stepwise, yielding $MoO_3 \cdot H_2O$ at 80–100° C and MoO_3 above 200° C. On the other hand, the dehydration of the acid C phase containing a small amount of NH_4^+ ions takes place gradually with rise in temperature, while maintaining the original structure in a temperature range from 20 to 400° C, as has been shown previously [4]. Thus, it is observed that the dihydrate, not containing any ammonium ions, loses almost all the water molecules on heating above 160° C and is converted to MoO_3. Scanning electron

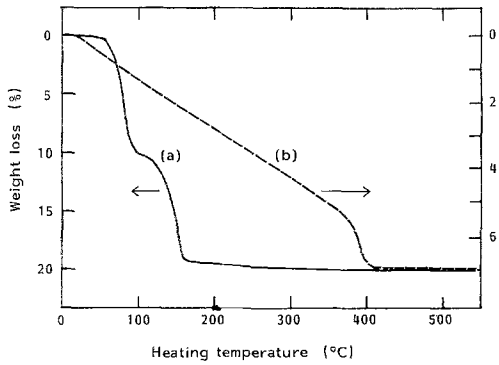

Fig. 1. Thermogravimetric curves of some molybdenum oxide hydrates. (a) $MoO_3 \cdot 2H_2O$ (number 1 in Table 1), (b) 0.075 $[(NH_4)_2O] \cdot MoO_3 \cdot 0.400(H_2O)$ (number 4). In air, heating rate 5° C min^{-1}.

micrographs of the dihydrate (number 1) and the acid C phase (number 4) and their heated products are given in Fig. 2, and the colour of these compounds is shown in Table 1. $MoO_3 \cdot 2H_2O$ (a) has a plate-like crystal form, while the acid C phase (d) has a different needle-like crystal form. These original crystal forms are observed to be maintained on heating up to 500° C, thus the crystal forms of the final products MoO_3 (c) and (e) are different from each other.

An a.c. complex impedance of molybdenum oxides (numbers 1–6 in Table 1) was measured in the frequency range from 10 mHz to 10 kHz at 25° C. The impedance plots of the dihydrate and its heated products (numbers 1, 2 and 3) formed a semi-circle with an associated capacitance of about 65, 170 and 167 pF, respectively. On the other hand, the C phase containing a small amount of ammonium ion and its heated products (numbers 4, 5 and 6) showed a different characteristic curve; a frequency spike with an associated capacitance of about 70, 250, and 530 pF was observed in numbers 4, 5 and 6, respectively. The electric conductivities obtained from the complex impedance planes are given in Table 1. All the molybdenum compounds (numbers 1–6) show a low conductivity of 10^{-11}–$10^{-8}\,\Omega^{-1}\,cm^{-1}$, and the conductivities of the trioxides of numbers 3 and 6 are found to be different by three orders of magnitude. The pellets obtained by combining the molybdenum compounds with graphite in a weight ratio of 1 : 1 showed a high conductivity of $10^{-2}\,\Omega^{-1}\,cm^{-1}$. Therefore the combined pellets were used for an electrochemical measurement.

3.2. *Electrochemical behaviour of the molybdenum oxide hydrate cathodes*

Typical discharge and recharge curves of several molybdenum oxide hydrates and their heated products are shown in Fig. 3. It can be seen from the figure that the hydrates $MoO_3 \cdot 2H_2O$ and $MoO_3 \cdot H_2O$ show a similar discharge behaviour, giving a discharge capacity of 350–400 Ah/kg-acid and a practical energy density of 850–1000 Wh/kg-acid corresponding to 2.4–2.5 electrons per mole of oxide. They show a stepwise discharge behaviour, including

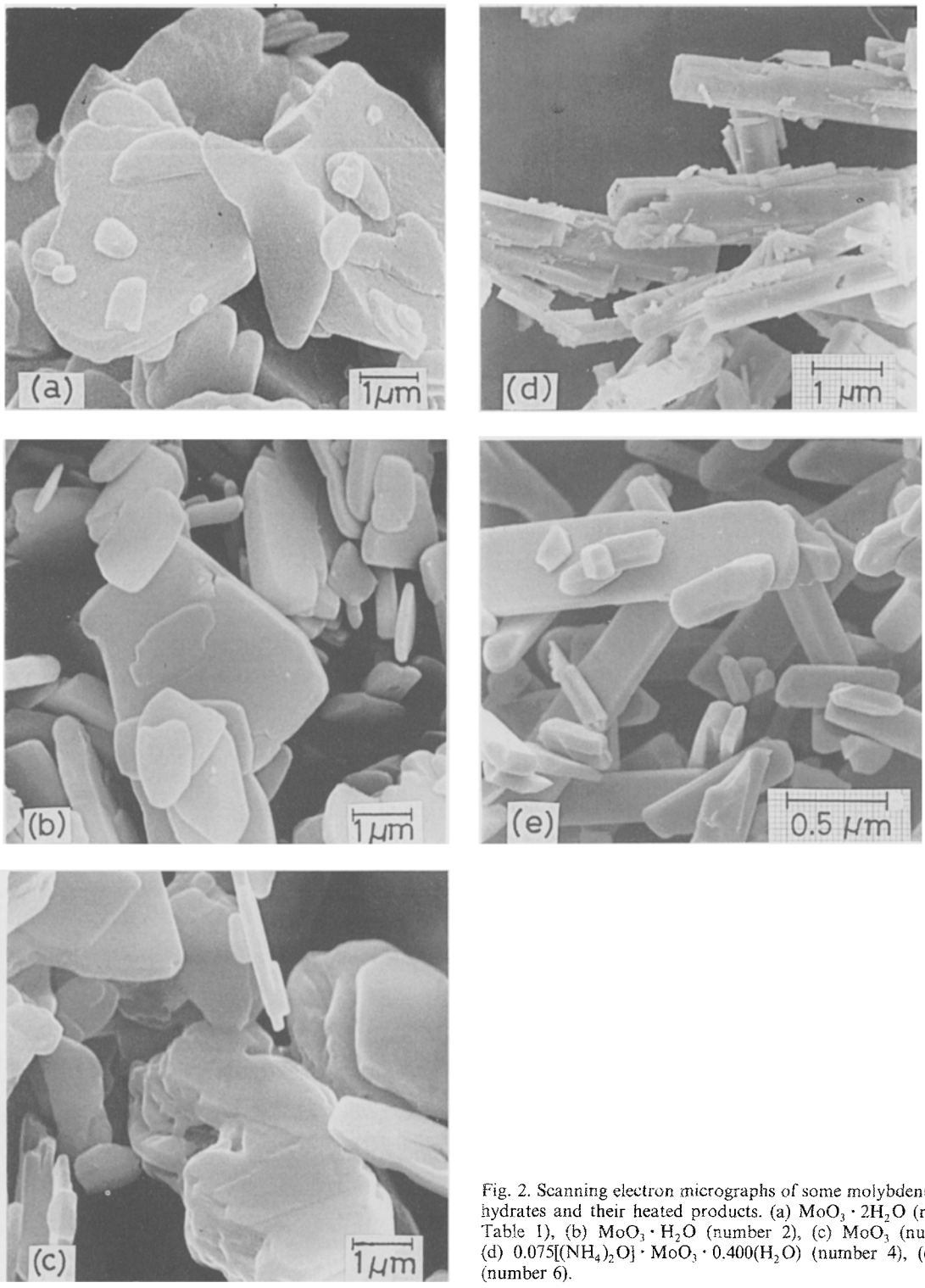

Fig. 2. Scanning electron micrographs of some molybdenum oxide hydrates and their heated products. (a) $MoO_3 \cdot 2H_2O$ (number 1 Table 1), (b) $MoO_3 \cdot H_2O$ (number 2), (c) MoO_3 (number 3), (d) $0.075[(NH_4)_2O] \cdot MoO_3 \cdot 0.400(H_2O)$ (number 4), (e) MoO_3 (number 6).

two plateaux; the first step up to $1e^-$/Mo and the second one up to $2e^-$/Mo. Anhydrous MoO_3, formed from $MoO_3 \cdot 2H_2O$ (c), gave a discharge capacity of 280 Ah/kg-oxide corresponding to $1.5e^-$/Mo. This value is in fair agreement with previous data of $1.3–1.6e^-$/Mo [1–3]. Both the anhydrous trioxides of numbers 3 and 6 in Table 1, formed from $MoO_3 \cdot 2H_2O$ and the C phase, showed a similar discharge behaviour, although their crystal forms and conductivities are very different. On the other hand, the C phase showed quite a flat curve, compared to the hydrates (a) and (b). When the $MoO_3 \cdot H_2O$ cathode (number 2 in Table 1) was discharged at various current densities (Fig. 4), the capacity decreased with increasing current density, reaching 300 Ah kg^{-1} at a high current density of 1 mA cm^{-2}. On discharge in several 1 M $LiClO_4$ solutions of PC and BL, the discharge behaviour was similar, but in DMSO the discharge potential in the second step decreased significantly (Fig. 5). Discharge of the cells with $MoO_3 \cdot 2H_2O$ (number 1), $MoO_3 \cdot H_2O$ (number 2) and MoO_3 (number 3) cathodes immediately after being filled with an electrolytic solution of 1 M $LiClO_4$–PC or after 30 days of storage were carried out at a constant current of 0.2 mA cm^{-2}. The capacity loss during storage was within 5% in all the cells. These results were in a good agreement with

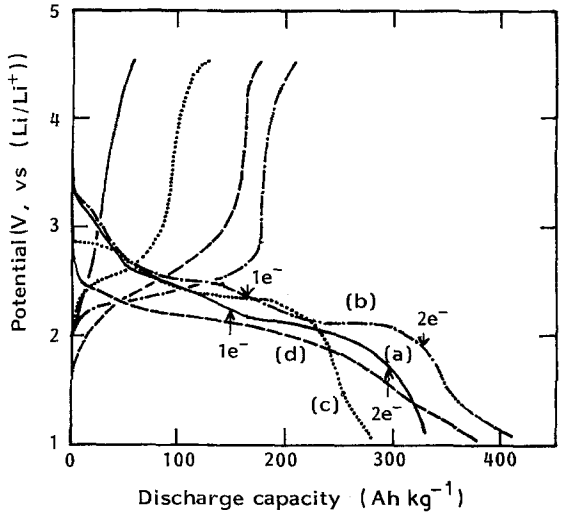

Fig. 3. Typical discharge curves of several molybdenum oxide hydrates and their heated products at a current density of 0.20 mA cm^{-2} and 25° C in 1 M $LiClO_4$–PC. (a) $MoO_3 \cdot 2H_2O$ (number 1 in Table 1), (b) $MoO_3 \cdot H_2O$ (number 2), (c) MoO_3 (number 3), (d) $0.075[(NH_4)_2O] \cdot MoO_3 \cdot 0.400(H_2O)$ (number 4).

the discharge result of the C phase (number 4) and MoO_3 (number 6) cells reported previously [4]. Thus, the capacity loss of $MoO_3 \cdot 2H_2O$ and $MoO_3 \cdot H_2O$ cells could not be attributed to the hydrated and coordinated waters in the structures of the oxides, but may be due to the trace impurities in the electrolyte.

The charge–discharge cyclic behaviour of $MoO_3 \cdot 2H_2O$ and its heated products (numbers 1–3 in Table 1) were examined. When they were first submitted to a deep discharge and then recharged up to the potential of 4.55 V vs Li/Li^+, as seen in Fig. 3, the recharge efficiencies of $MoO_3 \cdot H_2O$ and MoO_3 were about 50%, but that of $MoO_3 \cdot 2H_2O$ was about 20–25%, considerably lower than that of $MoO_3 \cdot H_2O$. This indicates that about 1 e$^-$/Mo of $MoO_3 \cdot H_2O$ is rechargeable. Therefore, the charge–discharge cyclings with the $MoO_3 \cdot H_2O$ cathode were carried out at constant capacities less than 1 e$^-$/Mo. The typical cyclic curves obtained at the capacity of 0.25 e$^-$/Mo is given in Fig. 6. It can be seen that the discharge potential decreases with an increasing cycling number, dropping to 1.1 V after 40 cycles. The polarization during charge is observed to increase with an increasing cycling number, which may limit the cycling number.

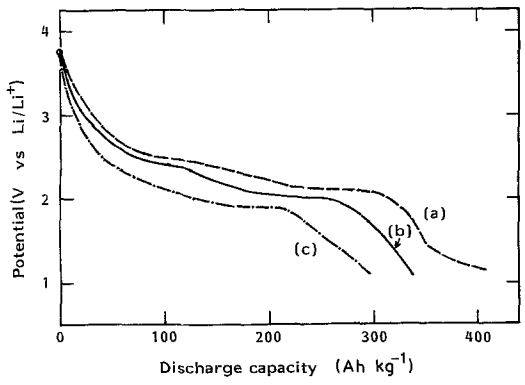

Fig. 4. Typical discharge curves of $MoO_3 \cdot H_2O$ cathode at several current densities in 1 M $LiClO_4$–PC. (a) 0.2 mA cm^{-2}, (b) 0.5 mA cm^{-2}, (c) 1 mA cm^{-2}.

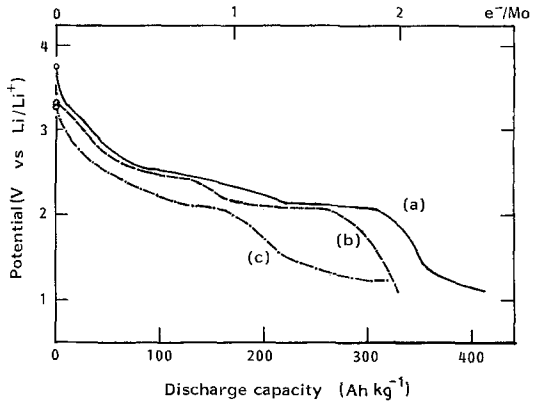

Fig. 5. Typical discharge curves of $MoO_3 \cdot H_2O$ cathode in various 1 M $LiClO_4$ electrolytic solutions at a constant current of 0.20 mA cm^{-2}. (a) PC, (b) BL, (c) DMSO.

3.3. *Structural changes in molybdenum oxide hydrates with discharge and recharge*

The structural changes in the oxides with discharge and recharge were at first followed using X-ray diffractometry. The structural relationships in the system $MoO_3 \cdot xH_2O$ (x = 0–2) are given schematically in Fig. 7. The powder X-ray diffraction patterns of $MoO_3 \cdot H_2O$ and its discharge and recharge products in 1 M $LiClO_4$–PC are shown in Fig. 8. $MoO_3 \cdot 2H_2O$ has a monoclinic system with lattice parameters of a = 0.377 nm, b = 0.691 nm, c = 0.734 nm and β = 90.4° [10] and it has both coordinated and hydrated water molecules and half of the water molecules act as hydrated water in the voids between layers [11]. The interlayer water molecules, bonding only through weak hydrogen bonds, are easily given off around 80° C to form $MoO_3 \cdot H_2O$ topotactically [12, 13]. $MoO_3 \cdot H_2O$ also has a monoclinic system with a = 0.755 nm, b = 1.069 nm, c = 0.728 nm and β = 91° and the layers are linked to each other through hydrogen bonds [12].

When $MoO_3 \cdot 2H_2O$ was discharged to 1 e$^-$/Mo

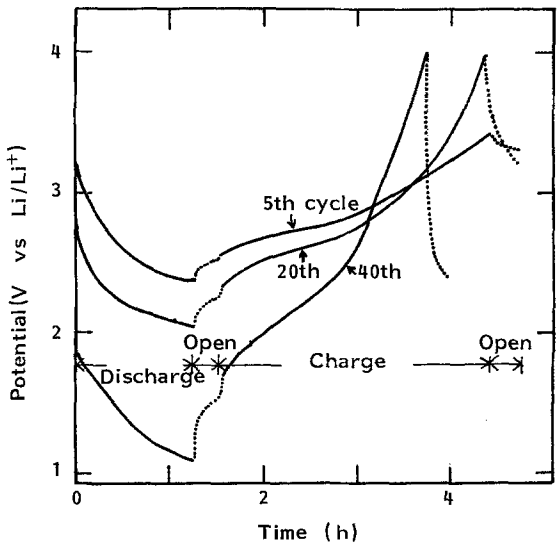

Fig. 6. Charge–discharge cyclic curves of $MoO_3 \cdot H_2O$ cathode in 1 M $LiClO_4$–PC. Discharge current 0.50 mA cm^{-2}, charge current 0.20 mA cm^{-2}. Cut off potential 1.10 V on discharge, 4.00 V on charge.

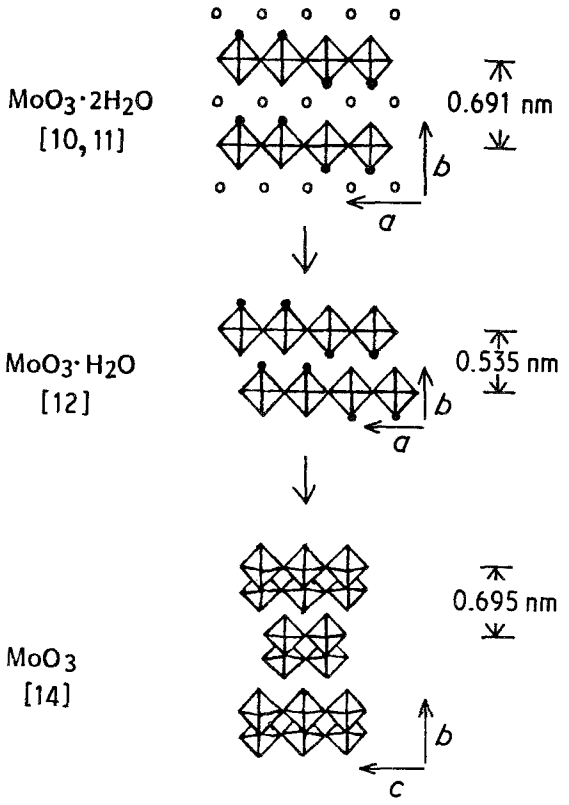

Fig. 7. Structural relationship in the system $MoO_3 \cdot H_2O$. o interlayer H_2O, ● coordinated H_2O, ◇ $[MoO_5(OH_2)]$ or $[MoO_6]$ octahedra.

in 1 M $LiClO_4$–PC, only (o n o) diffraction lines appeared as a broad peak and were shifed to considerably higher positions (2θ). This revealed that Li^+ ions are inserted between the layers with discharge,

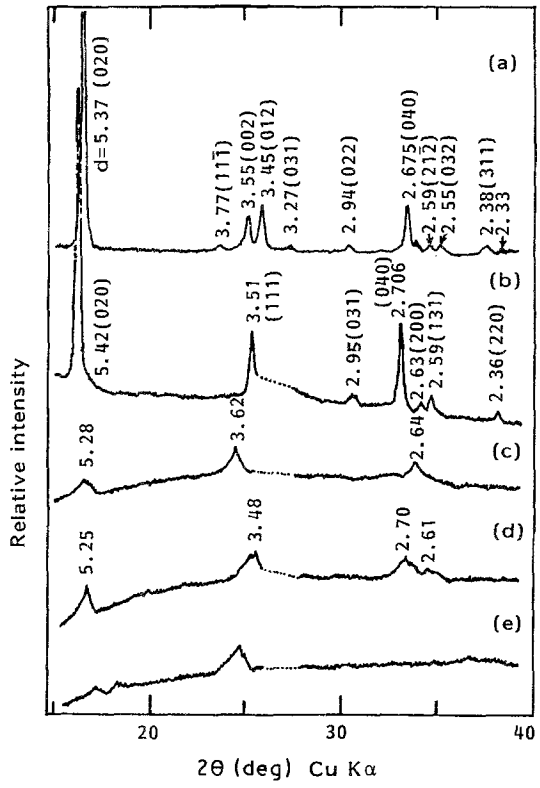

Fig. 8. X-ray diffraction patterns of $MoO_3 \cdot H_2O$ and its discharge and recharge products. (a) $MoO_3 \cdot H_2O$, (b) 0.5 e^-/Mo discharge, (c) 1 e^-/Mo discharge, (d) recharge after 1 e^-/Mo discharge, (e) 2 e^-/Mo discharge.

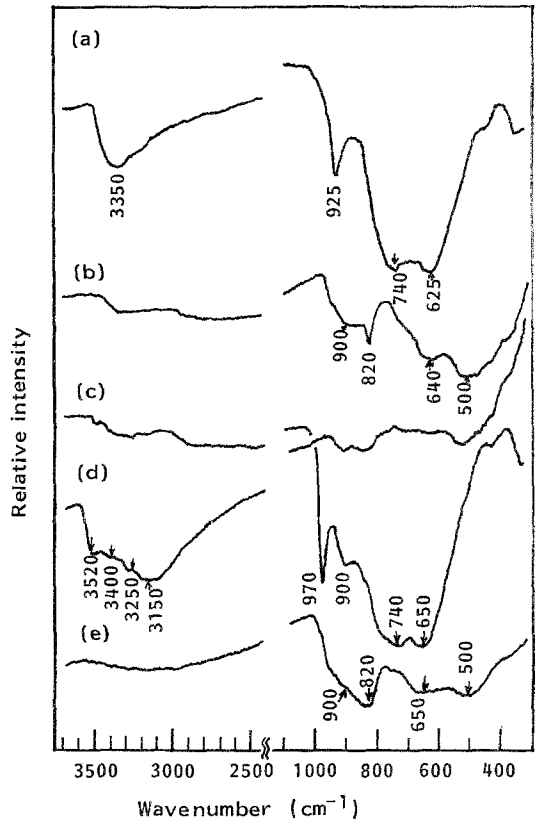

Fig. 9. Infrared spectra of some molybdenum oxide hydrates and their discharge products. (a) $MoO_3 \cdot H_2O$, (b) Discharge (a) to 1.0 e^-/Mo, (c) Discharge (a) to 2.0 e^-/Mo, (d) $MoO_3 \cdot 2H_2O$ (e) Discharge (d) to 1.0 e^-/Mo discharge.

resulting in a significant decrease in the layer spacing from 0.691 nm to 0.528 nm, corresponding to a decrease of 24 %. The layer spacing of the discharge product is found to be quite near that of $MoO_3 \cdot H_2O$ (b). On recharge after 1 e^-/Mo discharge, and after discharge to 2 e^-/Mo, the structures of the products were changed to an almost amorphous form. On the other hand, when $MoO_3 \cdot H_2O$ was discharged to 0.5–1.0 e^-/Mo, and then recharged, the X-ray patterns remain largely unchanged (Fig. 8), indicating that the original layered structure is maintained during the intercalation of Li^+ ions between layers. On discharge to 2 e^-/Mo, the structure become amorphous. All diffraction peaks except a weak one at 50.65° in the X-ray diffraction pattern of $MoO_3 \cdot H_2O$ (b) could be indexed on the basis of an orthorhombic unit cell of dimension a = 0.5285 nm, b = 1.0824 nm, c = 0.5237 nm. Thus, the structure of $MoO_3 \cdot H_2O$ was found to be changed from monoclinic to orthorhombic on the intercalation of Li^+ ions. On the other hand, as has been shown previously [4], the acid C phase showed a different heterogeneous reaction on discharge, resulting in a flat discharge potential in the region from 0.1 to 1 e^-/Mo. On discharge of $MoO_3 \cdot H_2O$ to 0.5 e^-/Mo in different 1 M $LiClO_4$ solutions of BL and DMSO, almost the same structural change was observed. The open circuit potentials (OCV) of the $MoO_3 \cdot H_2O$ cathode were measured in 1 M $LiClO_4$ solutions of PC, BL and DMSO after standing for 24 h at 25° C after discharge to 0.5 e^-/Mo. The OCVs observed were almost constant in the

range 2.49–2.58 V vs Li/Li^+ in all the solvents. Thus, the structural and thermodynamic studies indicate that unsolvated Li^+ ions are inserted between the layers during discharge up to $1\,e^-/Mo$.

Structural changes were further investigated using the IR spectrum (Fig. 9). $MoO_3 \cdot H_2O$, having only coordinated water, give one broad peak, assigned to OH stretching vibration at $3350\,cm^{-1}$, while in the case of $MoO_3 \cdot 2H_2O$, having both hydrated and coordinated water molecules, at least four peaks were observed in the frequency region $3000–3500\,cm^{-1}$. The IR spectra of these oxides were in fair agreement with the spectra shown by Günter [12]. On discharge with $MoO_3 \cdot H_2O$ to $1–2\,e^-/Mo$, the IR spectrum was changed considerably; the peak at $3350\,cm^{-1}$ lost intensity and broadened, and several peaks in the region from 500 to $1000\,cm^{-1}$, corresponding to Mo–O vibrations [15], in general shifted to lower frequencies (b and c). When $MoO_3 \cdot 2H_2O$ was discharged to $1\,e^-/Mo$ (e), the spectrum was also considerably changed, resulting in one highly similar to that of $MoO_3 \cdot H_2O$ discharged to $1\,e^-/Mo$ (b). These spectral results show that the Li^+ ions are inserted between the layers of the oxide, which would sever hydrogen bonds between layers. This would bring about a significant change in their spectra. In the case of the dihydrate, the Li^+ ions inserted may be combined directly with the interlayer water molecules, resulting in a significant decrease in the layer spacing as observed from the X-ray diffraction. Therefore, most of the Li^+ ions inserted may not be removed through a recharge process and an irreversible behaviour may be observed on charge–discharge cycling. In contrast to the dihydrate, $MoO_3 \cdot H_2O$, having only a coordinated water molecule, showed a good cycling behaviour within the capacity below $1\,e^-/Mo$, while keeping the original layered structure.

From a practical point of view, $MoO_3 \cdot H_2O$ with an energy density of 1000 Wh/kg-oxide and a high discharge potential of about 2.5 V vs Li/Li^+ may be considered as a promising cathode material for lithium batteries.

References

[1] F. W. Dampier, *J. Electrochem. Soc.* **121** (1974) 656.
[2] N. Margalit, *ibid.* **121** (1974) 1460.
[3] J. O. Besenhard and R. Schollhörn, *J. Power Sources* **1** (1976/1977) 267.
[4] N. Kumagai, N. Kumagai and K. Tanno, *Electrochim. Acta* **32** (1987) 1521.
[5] M. L. Freedman, *J. Amer. Chem. Soc.* **81** (1959) 3834.
[6] V. H. Peters, L. Till and K. H. Redeka, *Z. Anorg. Alleg. Chem.* **365** (1969) 14.
[7] M de L. Chaveg, P. Quintana and A. R. West, *Mater. Res. Bull.* **21** (1986) 1411.
[8] N. Kumagai and K. Tanno, *Denki Kagaku* **48** (1980) 601.
[9] N. Kumagai, K. Tanno and N. Kumagai, *Electrochim. Acta* **27** (1982) 1087.
[10] I. Linquist, *Acta Chem. Scand.* **4** (1950) 650.
[11] V. B. Krebs, *Acta Crystallogr.* **B28** (1972) 2222.
[12] J. R. Günter, *J. Solid State Chem.* **5** (1972) 354.
[13] H. R. Oswald, J. R. Günter and E. Dubler, *J. Solid State Chem.* **13** (1975) 330.
[14] G. Anderson and A. Magneli, *Acta Chem. Scand.* **4** (1950) 793.
[15] J. Selbin, *Angew. Chem. Intern. Edit.* **5** (1966) 712.